Reentrant Superconductivity Driven by Quantum Tricritical Fluctuations in URhGe: Evidence from ^{59}Co NMR in $URh_{0.9}Co_{0.1}Ge$

Y. Tokunaga,[1,*] D. Aoki,[2,3] H. Mayaffre,[4] S. Krämer,[4] M.-H. Julien,[4] C. Berthier,[4] M. Horvatić,[4] H. Sakai,[1] S. Kambe,[1] and S. Araki[2,5]

[1]*ASRC, Japan Atomic Energy Agency Tokai, Ibaraki 319-1195, Japan*
[2]*INAC/SPSMS, CEA-Grenoble/UJF, 38054 Grenoble, France*
[3]*IMR, Tohoku University, Ibaraki 311-1313, Japan*
[4]*LNCMI, UPR 3228, CNRS-UJF-UPS-INSA, 38042 Grenoble, France*
[5]*Department of Physics, Okayama University, Okayama 700-8530, Japan*

(Received 20 February 2015; published 27 May 2015)

Our measurements of the ^{59}Co NMR spin-spin relaxation in $URh_{0.9}Co_{0.1}Ge$ reveal a divergence of electronic spin fluctuations in the vicinity of the field-induced quantum critical point at $H_R \approx 13$ T, around which reentrant superconductivity (RSC) occurs in the ferromagnetic heavy fermion compound URhGe. We map out the strength of spin fluctuations in the (H_b, H_c) plane of magnetic field components and show that critical fluctuations develop in the same limited region near the field H_R as that where RSC is observed. This strongly suggests these quantum fluctuations as the pairing glue responsible for the RSC. The fluctuations observed are characteristic of a tricritical point, followed by a phase bifurcation toward quantum critical end points.

DOI: 10.1103/PhysRevLett.114.216401 PACS numbers: 71.27.+a, 74.25.nj, 74.40.Kb, 74.70.Tx

The occurrence of superconductivity in an itinerant ferromagnet, with the same electrons involved in both types of phase transition, is a counterintuitive idea. It is only during the past decade that such a paradox has found realization in a new family of uranium (U) based heavy fermion compounds, namely, UGe_2 [1], URhGe [2], and UCoGe [3]. Among these, URhGe is by far the most intriguing: Reentrant superconductivity (RSC) appears when a magnetic field of the order of 12 T is applied along the b axis, that is, perpendicular to the c axis direction along which the U $5f$ spin moments align ferromagnetically with a strong Ising character at zero field [4]. At a critical field $H_R \approx 12$ T, the ferromagnetic (FM) order is forced to align along the field direction ($\|b$). This quantum phase transition is strongly reminiscent of the textbook example of an Ising chain in a transverse field [5,6] and is considered to be responsible for the emergence of RSC [4,7–11], a trend that is by now well established in condensed matter physics. On theoretical grounds, it has been argued that ferromagnetic fluctuations provide the pairing glue in this new type of superconducting state [12,13], but microscopic experimental evidence is still lacking. Moreover, since the critical point at H_R is not an ordinary quantum critical point (QCP) but suggested to be a tricritical point (TCP) [4,8] followed by a phase bifurcation towards quantum critical end points (QCEPs), the nature of the spin fluctuations is thus expected to be different and more complex. In order to elucidate the microscopic nature of these fluctuations and their relationship with RSC, we have undertaken a ^{59}Co NMR study on a single crystal of $URh_{0.9}Co_{0.1}Ge$.

In pure URhGe, at zero magnetic field, U moments of $\sim 0.4\mu_B$ are aligned ferromagnetically along the c axis below the Curie temperature $T_{\mathrm{Curie}} = 9.5$ K (Fig. 1) [2]. The transverse field H_b along the b axis gradually decreases the temperature of the FM transition and eventually aligns the U moments along b at $H_R \approx 12$ T, resulting in a sudden jump of magnetization in a narrow field range (i.e., metamagnetism) [4,7,14]. Superconductivity (SC) emerges below $T_{\mathrm{sc}} \sim 0.25$ K, coexisting with the FM order at zero field [2]. This lower field SC is easily suppressed by H_b around 2 T, but then RSC appears at fields near H_R (between 8 and $\approx$13.5 T) with a higher $T_{\mathrm{sc}} = 0.42$ K [4,8].

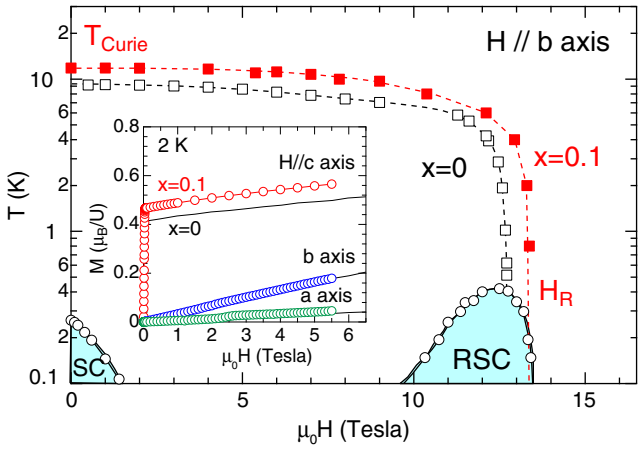

FIG. 1 (color online). Temperature-field phase diagram of $URh_{1-x}Co_xGe$. The inset shows the magnetization curves at 2 K.

Since both Rh and Ge nuclei have poor NMR sensitivity, we performed ^{59}Co NMR in $URh_{0.9}Co_{0.1}Ge$ [15]. The substitution of Co for Rh is isostructural and isoelectronic, and, while it precludes superconductivity (see Supplemental Material [17]), it only minimally affects the magnetic properties [19,20]. For example, $H_R(13.4\ \mathrm{T})$ and $T_{\mathrm{Curie}}(11.8\ \mathrm{K})$ are only slightly enhanced by Co substitution (Fig. 1), which suggests a small increase in magnetic correlations [19,20]. The spin system retains its strong Ising character along the c axis, and the magnetic susceptibility is strongly anisotropic even in the ab plain, as in pure URhGe [7] ($\chi_c > \chi_b > \chi_a$; see the inset in Fig. 1). Resistivity data are also similar to those previously reported for $x = 0$ (see Supplemental Material [17]). $URh_{0.9}Co_{0.1}Ge$ thus appears to be a suitable proxy, allowing us to probe with ^{59}Co NMR the microscopic nature of magnetic fluctuations in URhGe.

We used a high-quality single crystal of $URh_{0.9}Co_{0.1}Ge$, prepared by the Czochralski pulling method [2,11], to measure the field strength (H) and angle (θ) dependence of the nuclear spin-spin relaxation rate $1/T_2$, where θ is the angle from the b axis in the (bc) crystal plane, and the magnetic field components are thus $(H_b, H_c) = (H\cos\theta, H\sin\theta)$ [21]. The $1/T_2$ and the nuclear spin-lattice relaxation rate $1/T_1$ were measured for the central transition at the center of the NMR spectrum. All the NMR measurements reported here have been performed at $T = 1.6$ K, well below the T_{Curie} of 11.8 K of our crystals.

Figures 2(a) and (b) show ^{59}Co-NMR spectra in applied magnetic fields along the a and b axes. The magnetic susceptibility is very anisotropic even in the ab plane, and this can be directly visualized in the ^{59}Co NMR spectra: For $H\|a$, the spectrum [Fig. 2(a)] splits into seven sharp peaks, due to the quadrupolar interaction between the nuclear quadruple moment (spin 7/2) and the electric field gradient (EFG). For $H\|b$, on the other hand, the much larger Knight shift value of 19.6% (as compared to 2.9% for $H\|a$) increases the magnetic broadening by a factor of 3 (see Supplemental Material [17]). Therefore, the seven peaks merge into a single, broad, peak [Fig. 2(b)]. The blue lines are the result of NMR line simulation, assuming the same EFG anisotropy η and principal axes as those in UCoGe ([22–24] and see Supplemental Material [17]).

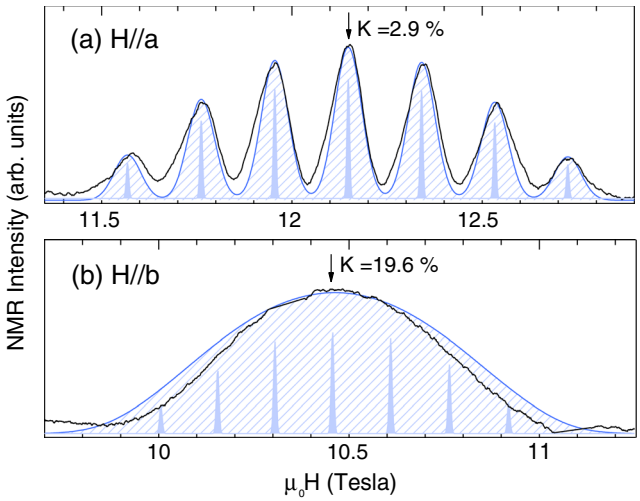

FIG. 2 (color online). ^{59}Co-NMR spectra in applied magnetic fields along the (a) a and (b) b axes at 1.6 K. The NMR spectra were recorded at fixed frequency by sweeping the magnetic field in equally spaced steps and by summing the Fourier transforms of the spin-echo signals measured with the $\pi/2$-τ-$\pi/2$ pulse sequence at each field value. The blue lines show the results of NMR line simulation (see the text).

The main result of this paper is the characterization of spin fluctuations as a function of the strength and the orientation of the magnetic fields, through measurements of the spin-spin relaxation rate $1/T_2$. $1/T_2$ is found to be field independent when the field is applied along the a axis, i.e., along the hardest magnetic axis [Fig. 3(a)], confirming the absence of any magnetic singularity, at least up to 17 T for $H\|a$. In contrast, $1/T_2$ for $H\|b$ shows strong field dependence associated with a divergence of magnetic susceptibility near H_R. The magnetic fluctuations become so strong near H_R that the NMR spin-echo signal is lost between 11.4 and 14 T, since T_2 values become shorter than the 3 μs dead time of the spectrometer. This divergence of $1/T_2$ near H_R is rapidly suppressed by tilting the field away from the b axis by an angle θ, i.e., by introducing an H_c component of applied field [Fig. 3(a)]: At $\theta > 5°$, the divergence is replaced by a broad maximum around 15.4 T, higher than for $\theta = 0$, which is around $H_R = 13.4$ T. $1/T_2$ thus shows a sharp maximum centered at $H_c = 0$ for $H = 11.2$ T, while for $H = 16$ T the maximum occurs at a finite value of $H_c \simeq 1.3$ T [Fig. 3(b)]. The latter behavior is related to a phase bifurcation above H_R, as discussed below.

The field-dependent $1/T_2$ observed here is associated with the longitudinal ($\|H$) component of spin fluctuations at zero frequency [25]. In general, $1/T_2$ is given by the sum of electronic and nuclear contributions: $1/T_2 = (1/T_2)^{\mathrm{el}} + (1/T_2)^{\mathrm{nu}}$. Here, we can safely assume that $(1/T_2)^{\mathrm{el}} \gg (1/T_2)^{\mathrm{nu}}$, since the nuclear spin-spin coupling among diluted Co nuclei is very small. Furthermore, the electronic contribution consists of two terms: $(1/T_2)^{\mathrm{el}} = (1/T_2)^{\mathrm{el}}_{\|} + (1/T_2)^{\mathrm{el}}_{\perp}$ with $(1/T_2)^{\mathrm{el}}_{\|} \propto G_{\|}(0)$ and $(1/T_2)^{\mathrm{el}}_{\perp} \propto G_{\perp}(\omega_{\mathrm{NMR}})$, where ω_{NMR} is the NMR frequency and $G_\alpha(\omega) = \int_{-\infty}^{\infty}\langle h_\alpha(t)h_\alpha(0)\rangle \exp(i\omega t)dt$ is the spectral density of the fluctuating hyperfine field $h_\alpha(t)$. Thus, $(1/T_2)^{\mathrm{el}}_{\|}$ is driven by the longitudinal component of magnetic fluctuations at zero frequency, while $(1/T_2)^{\mathrm{el}}_{\perp}$ is driven by the transverse ($\perp$) components of the fluctuations at the NMR frequency, still a very low value (~0.1 GHz). The latter fluctuations also generate the nuclear spin-lattice relaxation process $1/T_1$, which is related to $(1/T_2)^{\mathrm{el}}$ by the relationship $(1/T_2)^{\mathrm{el}}_{\perp} \simeq \beta(1/T_1)$ [26,27], where $\beta = 15.5$

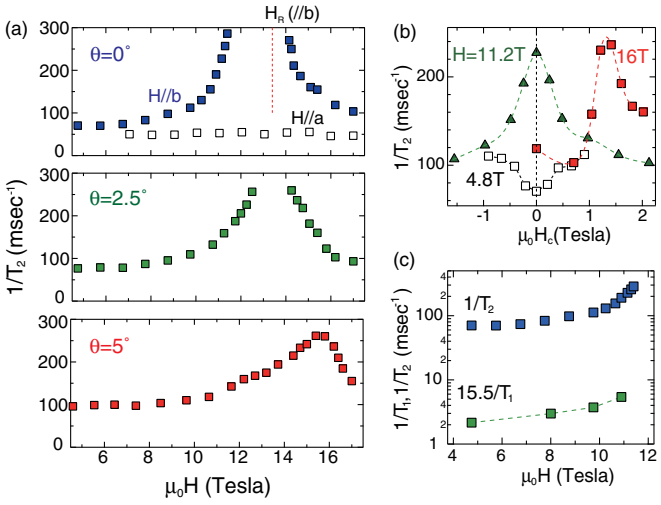

FIG. 3 (color online). (a) Field dependence of the relaxation rate $1/T_2$. (b) The H_c field component dependence of $1/T_2$ obtained by rotating the sample in applied fields of 4.8, 11.2, and 16 T. (c) Comparison of $1/T_1$ and $1/T_2$ for $H\|b$. The $1/T_2$ values were determined by fitting the τ dependence of the spin-echo intensity, measured at the center of the NMR spectrum, to an exponential function, $M(2\tau) \propto \exp(-2\tau/T_2)$. $1/T_1$ has been measured at the same position by the standard saturation-recovery method. All the data were taken at 1.6 K.

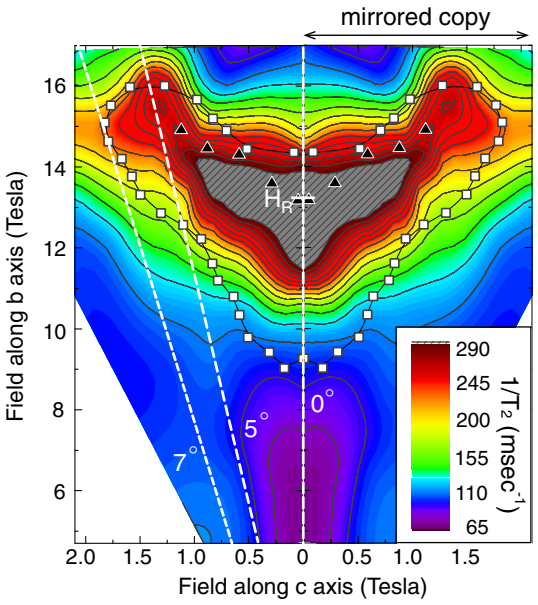

FIG. 4 (color online). Map of the magnetic fluctuation amplitude in the (H_b, H_c) plane around H_R. This contour plot of $1/T_2$ at 1.6 K is constructed from 104 data points measured with different combinations of H and θ values, between $H =$ 4.7 and 17 T and between $\theta = 0°$ and 11°, respectively. White dashed lines show constant-θ scans. The open squares indicate the region where RSC has been observed from resistivity measurements at $T \sim 40$ mK in a single crystal of URhGe [10]. The filled triangles indicate the first-order-like metamagnetic transitions at $T \sim 500$ mK [10]. Since URhGe has a lower H_R (12 T) than $URh_{0.9}Co_{0.1}Ge$ (13.4 T), these data for URhGe are plotted here with the field values scaled proportionally to the H_R values in $URh_{0.9}Co_{0.1}Ge$.

for the $m_z = -1/2 \leftrightarrow 1/2$ transition of $I = 7/2$ nuclei ([27] and see more details in Supplemental Material [17]). Therefore, one would expect $1/T_2 \simeq 15.5/T_1$ if $1/T_2$ were dominated by the $(1/T_2)^{\mathrm{el}}_{\perp}$ process. However, as seen in Fig. 3(c), we have observed $1/T_2 \gg 15.5(1/T_1)$ in the whole field range, indicating the dominance of the other, longitudinal, contribution to the $1/T_2$ process.

Our $1/T_2$ data are summarized in a contour plot on the (H_b, H_c) plane of the magnetic field components (Fig. 4). This shows how the critical fluctuations develop in the proximity of the H_R. The fluctuations are enhanced most strongly around H_R, where the NMR signal becomes undetectable due to the extremely short T_2 (hatched gray area). We also see the development of another weak singularity around $(H_b, H_c) \simeq (15.4\ \mathrm{T}, \pm 1.3\ \mathrm{T})$, which constitutes a clear signature of a phase bifurcation above H_R. Below, it is shown that these observations provide clear evidence for the tricritical nature of the transition.

In the transverse Ising system considered here, H_b and H_c are two distinct tuning parameters for the quantum phase transition: H_b controls the quantum fluctuations driving the phase transition itself, while H_c adds a perturbation conjugate to the order parameter, that is, the magnitude of FM moments along the Ising axis $\langle M_c \rangle$. Thus, we can expect two types of phase diagrams in the (H_b, H_c) plane, depending on the type of criticality. The phase diagram may simply involve a first-order planar surface for $H_c = 0$, bounded at finite temperature by a second-order transition line ending at the ordinary QCP at $T = 0$ [Fig. 5(a)]. The $H_c = 0$ long-range FM order is then everywhere continuously connected to the field-induced paramagnetic state [Fig. 5(b)]. On the other hand, a more rich and complex phase diagram appears if the system possesses a TCP, causing a bifurcation of the first-order planar surface at $H_c = 0$ into two wings that continue away from the H_b axis and end up at QCEPs at zero temperature for a finite H_c value [Fig. 5(c)]. The $H_c = 0$ projection is then discontinuous at the TCP [Fig. 5(d)]. Clearly, our observations in Fig. 4 support this latter case.

The emergence of diverging *longitudinal* fluctuations near H_R is another fingerprint of the presence of a TCP. Indeed, one of the characteristic features of a TCP with regard to magnetic excitations is that it triggers a diverging susceptibility not only for the order parameter but also for the physical quantity that is conjugate to the tuning parameter H_b driving the phase transition [9,28,29], namely, $\langle M_b \rangle$ in the present case. The presence of the TCP thus leads to a divergence of the longitudinal ($\|b$) component of magnetic fluctuations, giving rise to the observed very short $1/T_2$ [Figs. 5(c) and 5(d)]. This is not the case for an ordinary QCP, which induces solely the diverging susceptibility of the order parameter, i.e., the

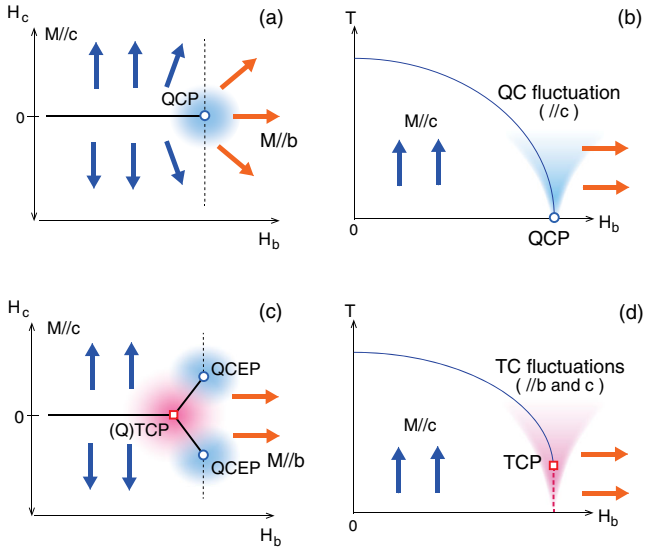

FIG. 5 (color online). (a) The H_b-H_c phase diagram involves a first-order transition planner surface at $H_c = 0$, which terminates at the QCP. The direction of the spontaneous FM moments (blue arrows) changes sign discontinuously when this surface is crossed. Dotted lines denote the crossover line passing through the QCP, which divides the paramagnetic state polarized along the b axis (red arrows) from the spontaneous FM ordered state along the c axis. (b) The first-order transition surface is delimited by a second-order FM transition (blue) line, continuously connected to the field-induced paramagnetic state at a single QCP (blue circle). (c) The first-order transition surface at $H_c = 0$ may bifurcate into two wings at the TCP, which end up at zero temperature at two QCEPs (blue circles). (d) Considering only the $H_c = 0$ plane, the TCP terminates the second-order phase transition line by a first-order transition (red dotted line).

divergence of the transverse fluctuations along the c axis [Figs. 5(a) and 5(b)]. A schematic phase diagram involving a TCP has already been proposed for URhGe; however, it mostly relied on the observation of first-order-like behavior near H_R [8,9,30,31]. The present NMR data go further, since they provide microscopic evidence of the existence of this TCP by probing directly the nature of the associated fluctuations.

Next, we focus on the mechanism of the reentrant superconductivity. In Fig. 4, we plot the region where the RSC has been observed in resistivity measurements by Lévy *et al.* in a single crystal of URhGe [10]. Obviously, the RSC occurs in almost the same region as that where we have observed the critical enhancement of fluctuations. This close interplay between the RSC and the fluctuations provides strong evidence that *the RSC is actually induced by these critical fluctuations around* H_R, most probably by reinforcing the pairing interactions [12,13]. The RSC has been known to be extremely sensitive to the field alignment; only about $\theta = 7°$ misorientation suppresses the RSC [10,32], and our results (Fig. 4) indicate that such suppression is definitely connected to the rapid decline of the critical fluctuations for $\theta > 7°$. The RSC has also been known to exhibit the highest T_{sc} and the largest diamagnetic signal just around H_R [4,14], where we have detected the diverging fluctuations.

The evidence presented here suggests that URhGe possesses quantum tricriticality, associated with its low temperature TCP [8,9,33], and hence it develops strong longitudinal fluctuations perpendicular to the Ising axis (parallel to the applied field) at low temperature. However, our observation being dominated by the longitudinal $\omega = 0$ fluctuations near the TCP, we cannot quantify the transverse fluctuations, including those parallel to the Ising axis. We recall that the spectrum density of FM critical fluctuations may have strong frequency dependence, with $G(0) \gg G(\omega)$. Therefore, since $1/T_2$ contains both $G_{\parallel}(\omega = 0)$ and $G_{\perp}(\omega_{\mathrm{NMR}})$, it may be, e.g., naturally dominated by $G_{\parallel}(\omega = 0)$ even for isotropic fluctuations. A divergence of the fluctuations is expected, in principle, for both the longitudinal and transverse components near the TCP, and such a tricritical nature of the fluctuations should be key to understanding the RSC phenomena in URhGe.

So far, most theories of the Ising FM superconductors have treated a single type of excitations, i.e., magnetic fluctuations parallel to the spontaneous moment direction, along the Ising axis [13,24,34–36]. Our results, however, reveal that the situation is more complex, at least in URhGe, and cannot be interpreted with a single type of excitations, in particular, near the TCP where the RSC emerges. This calls for an extension of the theory by involving fluctuations perpendicular to the Ising axis, and, indeed, a very recent study in the frame of Landau phenomenological theory shows that the strong enhance in magnetic susceptibility corresponding to the longitudinal fluctuation stimulates reentrance of the superconductivity near the first-order transition line [12].

We are grateful for stimulating discussions with R. E. Walstedt, J. Flouquet, N. Tateiwa, K. Hattori, H. Ikeda, K. Aoyama, and V. P. Mineev. A part of this work was supported by Japan Society for the Promotion of Science (JSPS) KAKENHI Grant No. 26400375, an European Research Council (ERC) starting grant (NewHeavyFermion), International Collaboration Center of Institute for Material Research (ICC-IMR) of Tohoku University, and the REIMEI Research Program of Japan Atomic Energy Agency (JAEA).

*tokunaga.yo@jaea.go.jp

[1] S. S. Saxena *et al.*, Nature (London) **406**, 587 (2000).
[2] D. Aoki, A. Huxley, E. Ressouche, D. Braithwaite, J. Flouquet, J.-P. Brison, E. Lhotel, and C. Paulsen, Nature (London) **413**, 613 (2001).
[3] N. T. Huy, A. Gasparini, D. E. de Nijs, Y. Huang, J. C. P. Klaasse, T. Gortenmulder, A. de Visser, A. Hamann, T. Görlach, and H. v. Löhneysen, Phys. Rev. Lett. **99**, 067006 (2007).

[4] F. Lévy, I. Sheikin, B. Grenier, and A. Huxley, Science **309**, 1343 (2005).
[5] See, for example, S. Sachdev, *Quantum Phase Transitions* (Cambridge University Press, Cambridge, England, 1999).
[6] A. W. Kinross, M. Fu, T. J. Munsie, H. A. Dabkowska, G. M. Luke, S. Sachdev, and T. Imai, Phys. Rev. X **4**, 031008 (2014).
[7] F. Hardy, D. Aoki, C. Meingast, P. Schweiss, P. Burger, H. v. Löhneysen, and J. Flouquet, Phys. Rev. B **83**, 195107 (2011).
[8] F. Lévy, I. Sheikin, and A. Huxley, Nat. Phys. **3**, 460 (2007).
[9] A. D. Huxley, S. J. C. Yates, F. Lévy, and I. Sheikin, J. Phys. Soc. Jpn. **76**, 051011 (2007).
[10] F. Lévy, I. Sheikin, B. Grenier, C. Marcenat, and A. Huxley, J. Phys. Condens. Matter **21**, 164211 (2009).
[11] A. Miyake, D. Aoki, and J. Fluquet, J. Phys. Soc. Jpn. **77**, 094709 (2008).
[12] V. P. Mineev, Phys. Rev. B **91**, 014506 (2015).
[13] K. Hattori and H. Tsunetsugu, Phys. Rev. B **87**, 064501 (2013).
[14] D. Aoki and J. Flouquet, J. Phys. Soc. Jpn. **83**, 061011 (2014).
[15] ^{59}Co nuclei possess a high nuclear spin value ($I = 7/2$) with quadrupole moment ($Q = 42$ fm^2) [16] and a relatively large nuclear gyromagnetic ratio ($\gamma_N = 10.03$ MHz/T), providing high efficiency of the NMR excitation pulses as well as high sensitivity of NMR detection. These advantages enabled the use of very short NMR pulses ($\sim 1\ \mu$sec), which was necessary to trace the spin-echo decay with extremely short T_2.
[16] R. K. Harris, E. D. Becker, S. M. C. De Menezes, R. Goodfellow, and P. Granger, Pure Appl. Chem. **73**, 1795 (2001).
[17] See Supplementary Material at http://link.aps.org/supplemental/10.1103/PhysRevLett.114.216401 for details on the effect of Co substitution, the resistivity measurements, the NMR line simulations and the relation between the NMR relaxation rates, which includes Ref. [18].
[18] W. Knafo, T. D. Matsuda, D. Aoki, F. Hardy, G. W. Scheerer, G. Ballon, M. Nardone, A. Zitouni, C. Meingast, and J. Flouquet, Phys. Rev. B **86**, 184416 (2012).
[19] S. Sakarya, N. T. Huy, N. H. van Dijk, A. de Visser, M. Wagemaker, A. C. Moleman, T. J. Gortenmulder, J. C. P. Klaasse, M. Uhlarz, and H. v. Löhneysen, J. Alloys Compd. **457**, 51 (2008).
[20] N. T. Huy and A. de Visser, Solid State Commun. **149**, 703 (2009).
[21] The hyperfine coupling tensors, relating the spin polarization at U sites to the hyperfine field observed at Co nuclei, is positive and nearly isotropic [22–24]. As a consequence, the hyperfine field fluctuations measured through $1/T_2$ of Co nuclei directly reflect the fluctuations of the U electronic spins and their anisotropy.
[22] T. Ohta, Y. Nakai, Y. Ihara, K. Ishida, K. Deguchi, N. K. Sato, and I. Satoh, J. Phys. Soc. Jpn. **77**, 023707 (2008).
[23] Y. Ihara, T. Hattori, K. Ishida, Y. Nakai, E. Osaki, K. Deguchi, N. K. Sato, and I. Satoh, Phys. Rev. Lett. **105**, 206403 (2010).
[24] T. Hattori *et al.*, Phys. Rev. Lett. **108**, 066403 (2012).
[25] In this Letter, "longitudinal" and "transverse" are defined with respect to the applied magnetic field. That is, longitudinal fluctuations are those along the b axis near the QCP, which is perpendicular to the "Ising" c axis.
[26] R. E. Walstedt, Phys. Rev. Lett. **19**, 146 (1967); **19**, 816 (1967).
[27] M. Horvatić and C. Berthier, in *NMR Studies of Low-Dimensional Quantum Antiferromagnets, in High Magnetic Fields: Applications in Condensed Matter Physics and Spectroscopy*, edited by C. Berthier, L. P. Lévy, and G. Martinez (Springer, Berlin, 2002), pp. 191–210.
[28] T. Misawa, Y. Yamaji, and M. Imada, J. Phys. Soc. Jpn. **75**, 064705 (2006).
[29] T. Misawa, Y. Yamaji, and M. Imada, J. Phys. Soc. Jpn. **77**, 093712 (2008).
[30] D. Aoki, G. Knebel, and J. Flouquet, J. Phys. Soc. Jpn. **83**, 094719 (2014).
[31] H. Kotegawa *et al.*, J. Phys. Soc. Jpn. **84**, 054710 (2015).
[32] E. A. Yelland, J. M. Barraclough, W. Wang, K. V. Kamenev, and A. D. Huxley, Nat. Phys. **7**, 890 (2011).
[33] M. T. Mercaldo, I. Rabuffo, A. Naddeo, A. Caramico D'Auria, and L. De Cesare, Eur. Phys. J. B **84**, 371 (2011).
[34] V. P. Mineev, Phys. Rev. B **88**, 224408 (2013).
[35] V. P. Mineev, Phys. Rev. B **90**, 064506 (2014).
[36] Y. Tada, S. Fujimoto, N. Kawakami, T. Hattori, Y. Ihara, K. Ishida, K. Deguchi, N. K. Sato, and I. Satoh, J. Phys. Conf. Ser. **449**, 012029 (2013).